Available online at www.sciencedirect.com
ScienceDirect
Polymer 48 (2007) 7098–7112
polymer
www.elsevier.com/locate/polymer

Synthesis of graft polyacrylamide with responsive self-assembling properties in aqueous media

Laurence Petit, Carole Karakasyan, Nadège Pantoustier, Dominique Hourdet*

Laboratoire de Physico-Chimie des Polymères et des Milieux Dispersés, UMR 7615 (UPMC – CNRS – ESPCI), 10 rue Vauquelin, 75005 Paris, France

Received 24 July 2007; received in revised form 24 September 2007; accepted 24 September 2007
Available online 29 September 2007

Abstract

Graft copolymers with water-soluble backbones were prepared using two different routes: *grafting onto* and *grafting through* techniques. The corresponding syntheses, leading to ionic or non-ionic copolymers, are described here in detail and exemplified with various primary structures obtained by changing the chemical nature of the side chains or the grafting ratio. Depending on the polyelectrolyte or neutral character of water-soluble backbones, viscosity-concentration dependences were determined at room temperature in dilute and semi-dilute regimes. Upon heating, PNIPA grafts dehydrate and self-aggregate into hydrophobic microdomains which promote the formation of a physical network above 36 °C. The main features of the thermoassociating properties of the copolymers in aqueous solutions are described using different experimental approaches: rheology, calorimetry, NMR spectroscopy and neutron scattering.

Keywords: Responsive assemblies; Hybrid networks; Poly(*N*-isopropylacrylamide)

1. Introduction

Thermothickening polymers, which lead to a reversible increase of viscosity upon heating, have attracted attention in the past decade as a result of their original behaviour. They proved to be very interesting for numerous applications in polymer science, in particular oil recovery, paint industry, drug delivery systems [1]. The main application envisioned is to adjust the viscosity of aqueous fluids [2–5] and to design hydrogels [1,6]. These unusual properties were initially observed with semi-dilute solutions of cellulose derivatives, and then with poly(alkylene oxide) such as poly(ethylene oxide) [PEO] and poly(*N*-substituted acrylamide) derivatives such as poly(*N*-isopropylacrylamide) [PNIPA] [3]. In that case, the associations are induced by a lower critical solution temperature (LCST) type phase separation taking place at a local scale [7].

A copolymer widely investigated in our research group is PAA-*g*-PNIPA [8,9], which combines a water-soluble backbone, poly(sodium acrylate) [PAA] and LCST PNIPA side chains. These copolymers illustrated very nicely the concept of thermo-association (Scheme 1).

It has been demonstrated that the molecular weight of the backbone is one parameter, but the charge density of the main chain also has to be considered as it controls the magnitude of electrostatic repulsions. Thus, recent investigations on mixtures of silica nanoparticles and copolymer PAA-*g*-PNIPA

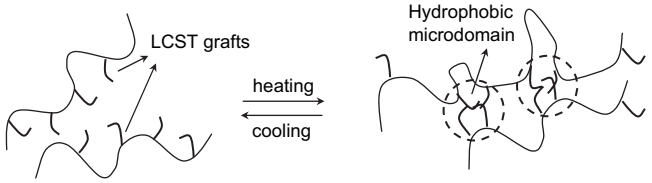

Scheme 1. Simplified view for a mechanism of thermothickening of graft copolymers. By heating, the LCST grafts undergo a microphase separation and create micelle-like aggregates which act as transient crosslinks.

* Corresponding author. Tel.: +33 (0)1 40 79 46 43; fax: +33 (0)1 40 79 46 40.
E-mail addresses: laurence_petit@hotmail.fr (L. Petit), carole.karakasyan@espci.fr (C. Karakasyan), nadege.pantoustier@espci.fr (N. Pantoustier), dominique.hourdet@espci.fr (D. Hourdet).

0032-3861/$ - see front matter © 2007 Elsevier Ltd. All rights reserved.
doi:10.1016/j.polymer.2007.09.040

at pH 8 raised the problem of electrostatic repulsions between silica surfaces (negatively charged at this pH) and copolymer backbones, which lead to long equilibrium times [10]. This main drawback leads us to develop new grafted structures based on weakly charged or neutral backbones issued from polyacrylamide chemistry. Moreover, in prospect of studying the rheological properties of hybrid networks prepared by mixing silica nanoparticles and graft copolymers, we synthesized a homologous series of graft macromolecules using either responsive or water-soluble side chains like PNIPA, PEO or poly(*N*,*N*-dimethylacrylamide); all of them being able to interact specifically with silanol groups.

For that purpose, we have considered two different strategies, on the one hand a peptide coupling between amino-terminated grafts and a modified polyacrylamide backbone (grafting onto) [4], and on the other hand, the way of a direct copolymerisation between acrylamide and an acrylamido macromonomer bearing the desired side chains (grafting through) [11].

The first protocol follows a four-step route: first, the synthesis of amino PNIPA [12,13] or PDMA grafts [14] (in the case of PEO, the corresponding amino-terminated graft is commercial, see Section 2), second the synthesis of the neutral PAM backbone, then its partial hydrolysis and finally the peptide coupling between the amino-terminated grafts and the backbone (see Scheme 2).

The second protocol also follows a multi-step route: first, the synthesis of amino PNIPA (or PDMA) grafts again, second a peptide coupling between acrylic acid and telomers which leads to an acrylamido macromonomer bearing PNIPA or PDMA side chains, third the copolymerisation between acrylamide and this macromonomer (see Scheme 3).

In the first part of this paper both routes leading to the synthesis of graft copolymers are described in detail. Then a comparative study concerning the rheological behaviour in dilute and semi-dilute regimes of copolymers containing PNIPA side chains is presented. Typical parameters such as intrinsic viscosities are determined and the concentration dependence of the viscosity is discussed taking into account the ionic or non-ionic nature of the backbone.

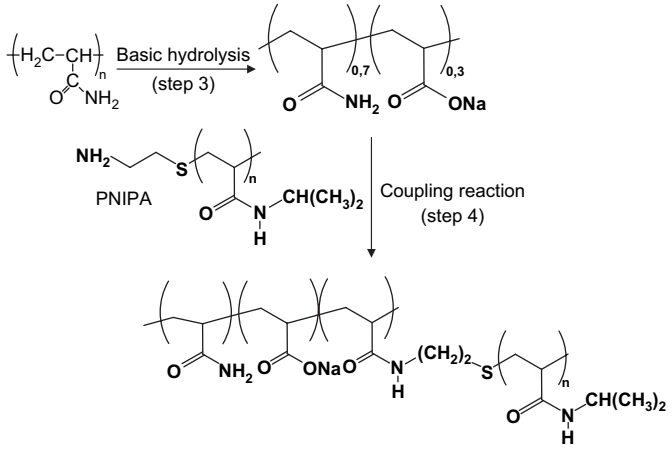

Scheme 2. Multi-step synthesis of graft copolymers: PAM-*g*-PNIPA (grafting onto route).

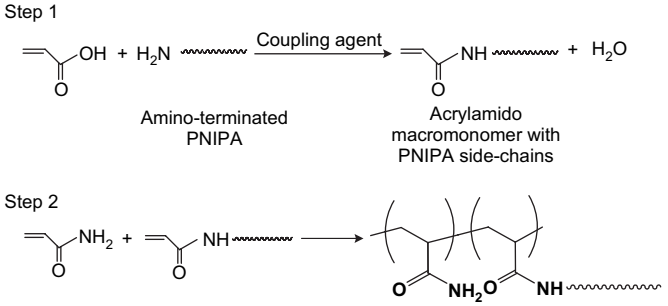

Scheme 3. Multi-step synthesis of graft polyacrylamide (grafting through route).

Finally, the thermothickening behaviour is investigated using various techniques such as rheology, calorimetry, SANS and NMR spectroscopy. Concerning the copolymers bearing PDMA or PEO side chains, the corresponding properties are not presented here since they do not self-associate in aqueous solution. Nevertheless, they easily form hybrid networks in the presence of silica nanoparticles and this will constitute the main topic of a forthcoming article.

2. Experimental section

2.1. Materials

Acrylamide (AM, 99% electrophoresis grade, Aldrich), acrylic acid (AA, anhydrous, Fluka), *N*-isopropylacrylamide (NIPA, 97%, Aldrich), *N*,*N*-dimethylacrylamide (DMA, 99%, Aldrich), cysteamine hydrochloride (Fluka), 3-mercaptopropionic acid (99%, Aldrich), potassium peroxodisulfate (Prolabo), ammonium peroxodisulfate (Merck), sodium metabisulfite (Prolabo), 2,2-azobis(2-methylpropionamidine)dihydrochloride (Kodak), *N*′,*N*′-dicyclohexylcarbodiimide (DCC, Aldrich) and 1-(3-dimethylaminopropyl)-3-ethylcarbodiimide hydrochloride (EDC, 98+%, Acros) were used as-received. Jeffamine M-2070, an amino-terminated poly(ethylene oxide-*co*-propylene oxide) [PEO] with 76 mol.% of ethylene oxide ($M_n \sim 1800\ g\ mol^{-1}$), was kindly supplied by Huntsman (Belgium). All organic solvents were of analytical grade and water was purified with a MILLIPORE system combining inverse osmosis membrane (Milli RO) and ion exchange resins (Milli Q).

2.2. Graft synthesis

Amino-terminated poly(*N*-isopropylacrylamide) [PNIPA] and amino-terminated poly(*N*,*N*-dimethylacrylamide) [PDMA] were prepared in the same conditions by telomerisation using cysteamine hydrochloride as telogen and potassium peroxodisulfate as initiator. The experimental conditions chosen are $R_0 = 0.01$ and $A_0 = 0.02$ with R_0 the molar ratio of monomer to initiator and A_0 the molar ratio of monomer to telogen. The protocol is described in Refs. [12,13] in the case of PNIPA telomers and can be summarised as follows.

In a three necked flask equipped with a reflux condenser, a magnetic stirrer and nitrogen feed, 10 g of NIPA (90 mmol) was dissolved in 100 mL of water and the solution was deoxygenated for 1 h with nitrogen bubbling. The initiators, KPS (0.9 mmol) and AET, HCl (1.8 mmol) were separately dissolved in 10 mL of water before addition to the NIPA solution. The reaction was allowed to proceed at a controlled temperature of 20 °C. After 4 h, an appropriate amount of sodium hydroxide was added to neutralise the hydrochloride ions and the polymer was recovered by dialysis against pure water (membrane cut-off = 6000–8000 Da) and freeze-drying. The reaction yield was 55%.

2.3. Copolymer synthesis by grafting onto (Scheme 2) technique

2.3.1. Poly(acrylamide) synthesis

Poly(acrylamide) [PAM] was obtained by free radical polymerisation in aqueous media, using 3-mercaptopropionic acid as transfer reagent and 2,2-azobis(2-methylpropionamidine)-dihydrochloride as initiator.

The polymerisation of AM was carried out in a three necked flask equipped with a reflux condenser, a magnetic stirrer and a nitrogen feed. Monomer (13 g, 0.182 mol) and transfer reagent (17.2–19.2 mg, 0.162–0.182 mmol) were dissolved in 600 mL of water and the resulting solution was deaerated for 1 h with nitrogen bubbling. The temperature was adjusted to 55 °C with a water bath and 0.507 g (1.82 mmol) of initiator, separately dissolved in 10 mL of deaerated water, was added under nitrogen atmosphere to the reaction medium. The reaction was allowed to proceed for 75 min at 55 °C followed by 75 min at 50 °C. Then the polymer solution was concentrated before precipitation in ethanol. The polymer was recovered by filtration and finally dried under vacuum. The final yield is 87%.

2.3.2. PAM partial hydrolysis

PAM was then partially hydrolysed (30 mol.% expected) to obtain a statistic copolymer [PAMH] of acrylamide and sodium acrylate.

The reaction was carried out in a three necked flask equipped with a reflux condenser, a magnetic stirrer and a nitrogen feed. PAM (11 g, 0.155 mol) was dissolved in 220 mL of water and 5.5 mL of isopropanol and the resulting solution was deaerated for 45 min with nitrogen bubbling. The temperature was adjusted to 45 °C with a water bath. Sodium hydroxide (1.86 g, 46.5 mmol) was separately dissolved in 10 mL of water, deaerated and added under nitrogen atmosphere to the reaction medium. The reaction was allowed to proceed for 20 h at 45 °C. Then the polymer solution was ultrafiltrated against pure water (membrane cut-off = 30 000 Da) and freeze-dried. The final yield is 89%.

2.3.3. Grafting reaction

In order to graft PNIPA, PDMA or PEO chains onto the PAMH backbone, we proceeded by peptide coupling using EDC as coupling reagent in water.

The grafting reaction was carried out at room temperature for PNIPA and PDMA and at 60 °C for PEO in a three necked flask where 5.0 g of PAMH and 5.0 g of PNIPA were added in 150 mL of water. The pH was adjusted at 7.3 and 10 equiv of EDC (relative to amine functions of amino-terminated graft) was added. The reaction was allowed to proceed for 2 h. Aliquots of about 1 mL were periodically sampled to follow the grafting reaction by SEC. After 1 h, the yield being quantitative, 300 mL of aqueous sodium chloride (0.2 mol L^{-1}) was added and the medium was stirred for 30 min. Then the polymer solution was purified by ultrafiltration against pure water (membrane cut-off = 30 000 Da) and recovered by freeze-drying. The corresponding graft copolymers are named PAMH-*g*-GRAFT(*x*), with *x* the weight percentage of graft in the copolymer.

2.4. Copolymer synthesis by grafting through (Scheme 3) technique

2.4.1. Synthesis of vinyl-terminated PNIPA

A peptide coupling between acrylic acid and amino-terminated PNIPA (or PDMA) was realized. The reaction was carried out at room temperature in a flask where 1.5 g of AA (0.021 mol), 9.0 g of PNIPA (around 1 mmol) and 4.1 g of DCC (0.021 mol) were added in 50 mL of methylene chloride. The reaction was allowed to proceed for 1 h under stirring. Dicyclohexylurea was removed by filtration. After precipitation in diethylene oxide, the polymer was finally recovered by filtration and dried under vacuum. The final yield is 65%.

2.4.2. Copolymerisation of acrylamide with the macromonomer

The following corresponds to a theoretical graft ratio of 30 wt.%. The reaction was carried out at room temperature in a three necked flask where 3.0 g of macromonomer, 7.0 g of AM and 7.8 mg of sodium metabisulfite (0.042 mol.% compared to AM) were added in 70 mL of water. The resulting solution was deaerated under stirring for 1 h with nitrogen bubbling. Then 31 mg of ammonium peroxodisulfate (0.14 mol.% compared to AM), separately dissolved in 5 mL of deaerated water, was added under nitrogen atmosphere to the reaction medium. The reaction was allowed to proceed for 4 h. Aliquots of about 1 mL were periodically sampled to follow the incorporation of the macromonomer by SEC. Afterwards, the polymer solution was purified by ultrafiltration against pure water (membrane cut-off = 30 000 Da) and recovered by freeze-drying. The corresponding copolymer containing PNIPA side chains are named PAM-*g*-PNIPA(*x*), with *x* the weight percentage of graft in the copolymer.

2.5. Analytical methods

2.5.1. Size exclusion chromatography (SEC)

Two different SEC instruments were used. The first one, which was mainly used for the characterisation of PAM samples, is equipped with two columns (Shodex OHpak SB-806 M HQ, $T = 40$ °C), a Waters 410 refractometer and a prototype

viscosimetric detector. The molar masses were derived from a universal calibration curve based on Pullulan standards from Sopares. The second one presents four OHpak columns and a differential refractive index detector (R401). It was used for samples containing PNIPA at 20 °C and only provides a qualitative monitoring of coupling reactions and polymerisations. For the two SEC systems, the flow rate was controlled at 1 mL min^{-1} using 0.5 M $LiNO_3$ as mobile phase.

2.5.2. Nuclear magnetic resonance (NMR)

^1H NMR (300 MHz) and ^{13}C NMR (75 MHz) spectra were recorded on a Bruker spectrometer. For temperatures higher than room temperature, the tubes were stabilized at the desired temperature in a water bath before analysis. In order to make quantitative comparisons between the spectra (at different temperatures), the integrations were normalized by the area of the peak of HOD at 25 °C.

2.5.3. Rheology

The viscosity analyses of dilute and semi-dilute aqueous polymer solutions were carried out at 20 °C on a Contraves Low Shear 30 rheometer equipped with stainless steel coaxial cylinders (radius of the cup: 6 mm, radius of the conical bob: 5.5 mm).

The viscosity analyses of aqueous graft copolymer solutions with temperature were carried out on a controlled stress rheometer (Haake RS150) using a cone/plate geometry. The temperature was adjusted by a high power Peltier system that provided fast and precise control of the temperature during heating and cooling stages. The experimental conditions were fixed at constant frequency and shear stress: 1 Hz and 5 Pa, respectively. A particular care has been taken to avoid drying of the sample by using a homemade cover which prevents from water evaporation during experiment. In these conditions, storage and elastic moduli as well as complex viscosity were recorded during temperature scans going from 20–60 °C (heating rate = 2 °C min^{-1}). Occasionally steady state viscosity measurements were also performed with the same rheometer by working in similar conditions at a fixed shear rate ($\dot{\gamma}^{-1} = 1$ or 10 s^{-1}).

2.5.4. Differential scanning calorimetry (DSC)

Thermograms were obtained using a Setaram MicroDSC III microcalorimeter by scanning between 20 and 70 °C at a heating rate of 1 °C min^{-1}. Using the temperature dependence of the heat flow, the endothermic peak can be integrated to obtain the cumulated enthalpy (H) as a function of temperature. The higher value of this cumulated enthalpy gives the transition enthalpy per NIPA repeat unit of the whole transition process H_t.

2.5.5. Small angle neutron scattering (SANS)

SANS experiments were performed at Laboratoire Léon Brillouin, Saclay (France). An incident neutron beam of wavelength $\lambda = 12$ Å was selected with a corresponding sample-to-detector distance of 4.6 m. This configuration provides a scattering vector modulus [$q = (4\pi/\lambda)\sin(\theta/2)$] ranging between 0.002 and 0.04 $Å^{-1}$ (where θ is the scattering angle). Polymer solutions were prepared at room temperature in D_2O and transferred into 2-mm thick quartz containers for SANS experiments. To obtain the coherent scattering intensity of the copolymer, the signal given by the solvent, used as background, was subtracted from the scattering intensity of the copolymer sample. The efficiency of the detector cell was normalized by the intensity delivered by a pure water cell of 1 mm thickness. Absolute measurements of the scattering intensity $I(q)$ (cm^{-1} or 10^{-8} $Å^{-1}$) were obtained from the direct determination of the incident neutron beam flow and the solid angle of the cell.

3. Results and discussion

3.1. Copolymer synthesis

3.1.1. Synthesis of precursors

3.1.1.1. α-Functionalised telomers. The preparation of functional poly(*N*-alkylacrylamide) has been carried out by a radical polymerisation mechanism initiated by a redox system ''CSH/KPS'' at room temperature (see Scheme 4).

Moreover, as the thiol is an efficient chain transfer reagent, it allows controlling the nature of the end groups of the chains as well as their molecular weight. On the basis of our expertise on telomerisation of NIPA [8], we used in the present study $R_0 = 0.01$ and $A_0 = 0.02$ which is a good compromise in order to get (1) a good control of the functionality and (2) intermediate molecular weights ($M_n = 6000$–$12\,000$ g mol^{-1}) which allow the design of graft copolymers with remarkable self-assembling properties. As a matter of fact, low molecular weight side chains generally weaken the strength of the physical network while very long grafts need oversized architectures with high molecular weight backbones in order to compromise over a reasonable number of grafts per chain (minimum 2) and a reasonable weight fraction of water-soluble material.

The amino-terminated telomers prepared in this study were characterised by ^1H NMR as reported in Fig. 1 for PNIPA. For chains of intermediate size, the integration of methylene groups of the CSH fragment introduced at one end, and visible between 2.4 and 3.6 ppm, can be used to determine the average molar mass of telomers. This was done for PNIPA which cannot be characterised by aqueous SEC at 40 °C (see Table 1). Conversely the molar masses of PDMA were determined by SEC rather than NMR as the molar fraction of CSH fragment in the polymer chain is much lower.

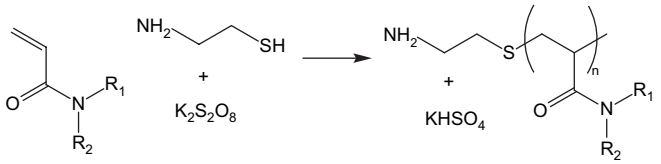

Scheme 4. Telomerisation of *N*-alkylacrylamide derivatives using aminoethanethiol (CSH) as chain transfer reagent and potassium peroxodisulfate (KPS) as co-initiator.

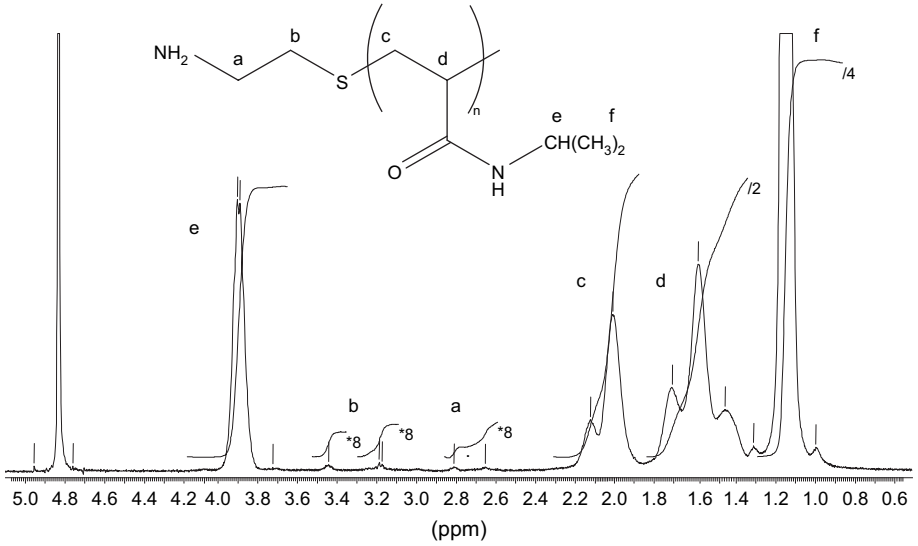

Fig. 1. ^{1}H NMR spectrum of PNIPA in D_2O at 20 °C: 3.9 ppm (C*H*, 1H), 3.45 ppm (CH_2SH, 2H), 3.2 ppm (NH_2CH_2, 2H), 2.0 ppm (C*H*, 1H), 1.6 ppm (CH_2, 2H), 1.1 ppm (CH_3, 6H).

PDMA is characterised by a number average molar mass $M_n = 11\,200$ g mol^{-1} ($DP_n = 113$) with a polydispersity index of 2 which is reasonable with this type of reaction. As the average degree of polymerisation of PDMA is 50% higher than PNIPA, while the conditions of synthesis remained the same, it can be concluded that the transfer efficiency is lower with DMA as compared to NIPA.

In the framework of the route ''grafting onto'', the terminal amine function was changed into a vinyl group in order to get a polymerisable macromonomer. The peptide coupling reaction was performed with a large excess of activated carboxyl, using 20 mol of DCC and 20 mol of COOH per mole of amine. The conversion was checked only qualitatively by ^{13}C NMR, but as this reaction can be considered as a tool of click chemistry, we can reasonably assume that the modification is quantitative. Advanced discussion on this point will be given, in Section 3.1.3.

3.1.2. Synthesis of hydrolysed polyacrylamide

Concerning the choice of AM polymerisation method, it is worth noting that initial attempts in controlled radical polymerisation, especially Atom Transfer Radical Polymerisation (ATRP) have been carried out. At that time and to our knowledge, there were only two examples of controlled radical polymerisation of AM by ATRP [15,16]. Jewrajka et al. have synthesized a polyacrylamide of relatively high molecular weight ($M_n \approx 4 \times 10^4$ g mol^{-1}) with a polydispersity index of about 1.5–1.9. Consequently, we tried to use an ATRP system based on a pentamethyldiethylenetriamine copper (I) complex in aqueous glycerol media to synthesize higher molecular weight PAM ($M_n \approx 7 \times 10^4$ g mol^{-1} expected). The first attempts led to very high molecular weights and broad polydispersities, which are typical of uncontrolled free radical polymerisation. Further results were suitable in terms of M_n but polydispersity indices still remained too large.

After these unsuccessful attempts, we tried to extend the telomerisation technique in the case of acrylamide. Using this method, we wanted to take advantage of the ability of the transfer reagent to temper the polymerisation, but the end-chain functionalization aspect was out of scope in that case.

First, we tried without success to use the same system initiator–transfer reagent as for the PNIPA synthesis, but we rapidly turn towards a new system composed of 2,2-azobis(2-methylpropionamidine)dihydrochloride as initiator and 3-mercaptopropionic acid as transfer reagent. After adjusting the different ratios, the reaction time and the temperature (see the protocol in Section 2), we were able to obtain PAM of intermediate molecular weights ($M_w = 100$–150 kg/mol) with reasonable polydispersity indices for a free radical polymerisation (PDI = 2.5–3; see Table 2).

Otherwise it is also interesting to notice that recently, McCormick et al. [17] have shown that the Reversible Addition-Fragmentation chain Transfer (RAFT) technique seemed to be the best way to control the polymerisation of AM and to synthesize quite high molecular weight polymers.

Table 1
Characterisation of polymer precursors

	M_n[a] (g mol^{-1})	DP_n[a]	PDI
PNIPA	8500	75	–
PDMA	11 200	113	2.0

[a] M_n determined by ^{1}H NMR for PNIPA and by SEC for PDMA.

Table 2
Synthesis and characterisation of PAM

Polymer	R_0[a]	M_w[b] (g mol^{-1})	DP_w[b]	PDI[b]
1-PAM	1.0×10^{-3}	122×10^3	1720	3.2
2-PAM	0.9×10^{-3}	144×10^3	2020	2.4

[a] R_0 is the molar ratio between the transfer reagent and the monomer.
[b] Determined by SEC.

After the polymerisation of acrylamide a partial hydrolysis of monomer units is necessary in order to introduce reactive groups (COOH) for the grafting of amino-terminated telomers. Preliminary experiments (not shown here) have pointed out that a hydrolysis rate lower than 30 mol.% does not allow a quantitative yield in the coupling reaction. This was also observed by Lloyd and Burns [18] and the rate was fixed to this value (30 mol.%).

The hydrolysis of PAM was performed at high pH following the experimental conditions described by Halverson et al. [19]. The hydrolysed samples (1-PAMH and 2-PAMH) were characterised by ^{13}C NMR in order to determine the true composition (31 and 33 mol.% of sodium acrylate units; respectively) and to investigate their microstructure (see Fig. 2).

Whatever the PAM, the results are very close to those obtained by Halverson et al. [19] and do not really correspond to a random spreading of the carboxyl groups along the backbone (see Table 3). The major difference lies in the fact that there are very few "BB" sequences and conversely more ABA triad than it can be calculated from the Bernoullian statistics (random distribution of A and B). As a matter of fact, it was shown [19] that contrary to acid hydrolysis of PAM which tends to develop blocks of carboxyl groups, mild alkaline hydrolysis provides a well-spaced distribution of carboxyl groups along the polymer chain. Mainly due to electrostatic repulsions, it is obviously less favourable to hydrolyse an amide group, and creating a new sodium carboxylate one, in the vicinity of another anionic monomer already hydrolysed.

3.1.3. Grafting onto technique

Amino-terminated PNIPA, PDMA or PEO was grafted onto PAMH backbones using carbodiimide chemistry. Except for the PEO grafting, which was performed at 60 °C as previously reported [4], the coupling reaction between PNIPA (or PDMA) and PAMH was investigated at room temperature. For this purpose, several conditions were tested (mainly pH and carbodiimide content) followed by SEC in order to ensure a quantitative coupling. From these preliminary studies, it was shown that a large number of carboxyl groups, by comparison with the total number of amines introduced, must be activated by EDC. An example is given in Fig. 3 in the case of PNIPA and 1-PAMH using a molar ratio "EDC/NH_2" of 10 (pH = 7.3). In that case, the grafting is almost quantitative in less than 1 h and the same conditions were successfully applied for the grafting of PNIPA and PDMA onto PAMH. The composition of graft copolymers obtained from ^{1}H NMR is reported in Table 4.

Due to the structure of these copolymers containing long side chains, we can see that a high weight fraction of grafts in the copolymer, between 40 and 70%, finally corresponds to a very small number of grafts (between 1 and 3%). Depending on the copolymer, this corresponds to an average of 30–110 monomer units between two grafts and by taking into account the number average degree of polymerisation of the main chain we get a better overview of the primary structure of the copolymers bearing between 7 and 16 grafts per backbone. Finally, considering (1) the well-spaced distribution of carboxyl units in the parent PAMH, (2) the steric hindrance between grafts during the coupling reaction and (3) the fact that the reaction was performed in homogeneous conditions, we can reasonably assume that the side chains are also well spaced along the backbone and the probability to find

Table 3
Assignment of ^{13}C NMR peaks of 1-PAMH (carbonyl region) to the different triads of the hydrolysed polyacrylamide (A = acrylamide, B = sodium acrylate)

	AAA	AAB	BAB	ABA	BBA	BBB
δ (ppm)	182.3	182.8	183.3	185.6	186.0	Not observed
$\%_{Exp}$	22	36	8	24	10	Not observed
$\%_{Exp}$ [a]	21	38	9	22	10	Not observed
$\%_{Random}$ [b]	34.3	29.4	6.3	14.7	12.6	2.7

[a] Experimental results obtained by Halverson et al. [19] with a hydrolysis rate equal to 33 mol.%.
[b] Theoretical calculations corresponding to a random spreading of A and B units in the case of a hydrolysis rate equal to 30 mol.%.

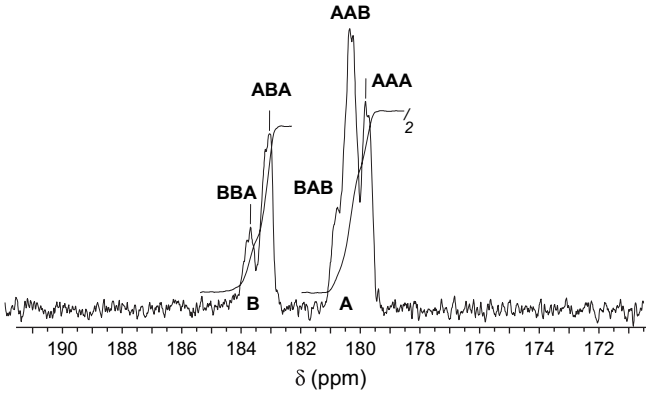

Fig. 2. Part of ^{13}C NMR spectrum of a solution of 1-PAMH in D_2O at 20 °C. 183 ppm (*CO*, sodium acrylate = B, int. 0.94), 180 ppm (*CO*, acrylamide = A, int. 2.06).

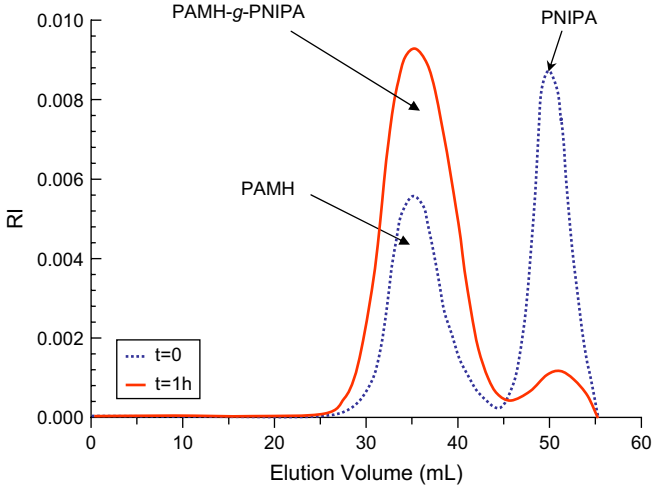

Fig. 3. Size exclusion chromatograms recorded at various reaction times for the coupling reaction between PNIPA and 1-PAMH ($T = 20$ °C, pH ≅ 7, EDC/NH_2 = 10). Dotted line corresponds to the time zero, full line corresponds to a reaction time of 1 h.

Table 4
Nomenclature and composition of copolymers obtained by grafting onto technique

Copolymer	w_g [a]	n_g [b]	N_g [c]
1-PAMH-*g*-PEO(40)	41	3	16
1-PAMH-*g*-PNIPA(60)	60	1.4	7
2-PAMH-*g*-PNIPA(50)	49	0.9	8
2-PAMH-*g*-PDMA(70)	70	1.6	14

[a] Weight percentage of graft in the copolymer.
[b] Average number of graft per 100 monomer units of the main chain.
[c] Average number of grafts per copolymer chain.

polymeric grafts anchored on neighbouring units can be ruled out. This cannot be proved experimentally as the molar fraction of graft is too low, but this was clearly evidenced for instance with the grafting of dodecylamine (20 mol.%) onto polyacrylic acid performed in homogeneous conditions (*N*-methylpyrrolidone) [20].

To conclude on this route, we can say that in spite of a long procedure involving four steps, it allows to prepare graft copolymers with rather well-defined architectures. The control of the primary structure during the different steps of the synthesis takes into account the size and the molecular weight distribution of the precursors (backbones and side chains) as well as the distribution of the grafts along the main chain.

3.1.4. Grafting through technique

The main difficulty when copolymerising two different monomers comes from their different reactivity. This behaviour could be even more pronounced for steric reasons when macromonomers are used, as they are generally less reactive than small monomers carrying similar vinyl group. Besides this main drawback, the advantage of copolymerisation is that this reaction can be applied to a wide range of comonomers, giving rise to a large variety of architectures. In the case of PNIPA macromonomers, SEC was used to follow the conversion of the polymerisation. In our experimental conditions, it was shown that while the polymerisation of acrylamide was quantitative after 4 h, a fraction of PNIPA remains unreacted. The composition of copolymers was characterised by NMR and the data are reported in Table 5.

For the polymerisations performed between AM and PNIPA (or PDMA), we can check that the incorporation of the macromonomer is not quantitative and remains especially low (around 30%) for the copolymerisation performed with the lower content of PNIPA. Moreover, we have to consider that if the initial weight ratio AM/macromonomer is relatively well balanced between the two monomers, between 1 and 2.3, it is far to be the case for the initial molar ratio AM/macromonomer which varies roughly between 120 and 320. Due to the large difference of reactivity between the two monomers and the large imbalance between their molar content, we also expect a significant composition drift of comonomers in the course of the reaction, giving rise to many different architectures from low grafted until high grafted copolymer chains. If we look at the average composition of the resulting copolymers, the frequency of grafting will range between 0.12 and 0.70%, values which are significantly lower compared to the previous PAMH series obtained by grafting onto.

Table 5
Composition of copolymers obtained by grafting through technique

Polymer	$\omega_{g,th}$ [a]	$\omega_{g,exp}$ [b]	n_g [c]
PAM-*g*-PNIPA(13)	30	13	0.1
PAM-*g*-PNIPA(46)	50	46	0.7
PAM-*g*-PDMA(25)	33	25	0.2
PAM-*g*-PDMA(46)	50	46	0.5

[a] Theoretical weight percentage of macromonomer in the copolymer calculated from the feed monomer ratio.
[b] Experimental weight percentage of macromonomer in the copolymer obtained by ^{1}H and ^{13}C NMR measurements.
[c] Average number of graft per 100 monomer units of the main chain.

We were not able to characterise the molar masses of PAM-*g*-PNIPA copolymers by SEC in water, due to the hydrophobic nature of PNIPA grafts at 40 °C, but this was possible for copolymers prepared in similar conditions with the hydrophilic macromonomer PDMA. The two PAM-*g*-PDMA samples reported in Table 5 were characterised by a broad distribution of their molecular weights ($M_w \cong 4-5 \times 10^5$ g mol^{-1}, PDI $\cong$ 6) and we can reasonably extrapolate close characteristics for PAM-*g*-PNIPA derivatives if we assume a similar reactivity between PNIPA and PDMA in the framework of their copolymerisation with acrylamide.

To conclude on this route, we can say that grafting through is an interesting alternative to diversify the chemical architecture of associating graft copolymers and to prepare non-ionic structures as we were looking for in the present work. Nevertheless, compared to the previous ''grafting onto'' series, the copolymer chains prepared by ''grafting through'' are not as well defined and exhibit at the same time a high polydispersity of the main chain and a broad distribution of their chemical composition.

In the following part of this paper, we will investigate the behaviour of these graft copolymers in aqueous solution in order to point out some important relations between the properties and the primary structure.

3.2. Viscosity of graft copolymer solutions at 20 °C

Before investigating of the viscoelastic properties of graft copolymers in aqueous solutions, mainly PNIPA derivatives, it is important to determine the different regimes of concentration.

3.2.1. PAM series

In the case of non-ionic copolymers, we first determine their intrinsic viscosity from low shear experiments performed on a wide range of concentration (C_p). For that purpose we apply Fedors [21] relation:

$$\frac{1}{2\left(\eta_r^{1/2}-1\right)} = \frac{1}{[\eta]}\left(\frac{1}{C_p}-\frac{1}{C_m}\right) \quad (1)$$

where η is the viscosity of the solution, η_S is the viscosity of the solvent, η_r is the relative viscosity ($\eta_r = \eta/\eta_S$) and C_m is

the concentration parameter which can be compared with the maximum packing fraction ϕ_m in the case of solid particles.

Initially developed to describe the viscosity of Newtonian suspensions of rigid particles, Fedors [21] has shown on the basis of a large set of experimental data that the above equation could be applied to a large variety of systems with relative viscosities ranging between 1 and 100. From Fedors plots given in Fig. 4, the intrinsic viscosity ([η]) can be extrapolated by linear regression for each copolymer: $[\eta] = 200$ mL/g for PAM-*g*-PNIPA(13) and $[\eta] = 360$ mL/g for PAM-*g*-PNIPA(46). A quantitative comparison between the two copolymers is not really obvious due to the lack of information concerning the molar masses of the samples. Nevertheless, we can simply compare the intrinsic viscosities just considering that [η] is proportional to the hydrodynamic volume of the chain (v) divided by its molar mass (M). For a backbone of given size, the volume of the chain generally increases with increasing grafting density but as at the same time the molar mass increases more rapidly the consequence is that [η] must decrease with increasing number of grafts, i.e. forming objects of increasing density.

In the present case we observe an opposite situation which is related to the lack of control of the molar mass of the chain and we can only conclude that the intrinsic viscosity of PAM-*g*-PNIPA(13) is lower than that of PAM-*g*-PNIPA(46) simply because the former has a lower molar mass.

Using the intrinsic viscosity of the copolymers, it is then possible to draw a master curve by plotting the specific viscosity ($\eta_{spe} = \eta_r - 1$) as a function of the reduced concentration $C_p[\eta]$ (see Fig. 5). From this curve, which is similar to the master curve reported by Grigorescu and Kulicke [22] with solution of polyacrylamide of various molar masses, we can point out the following features:

(1) the departure from dilute regime to unentangled semi-dilute regime occurs around $C^*[\eta] \cong \eta_{spe} \cong 1 - 2$. This well-known overlap criterion corresponds effectively to $C_p = 5$ and 10 g L^{-1} for PAM-*g*-PNIPA(46) and PAM-*g*-PNIPA(13), respectively.

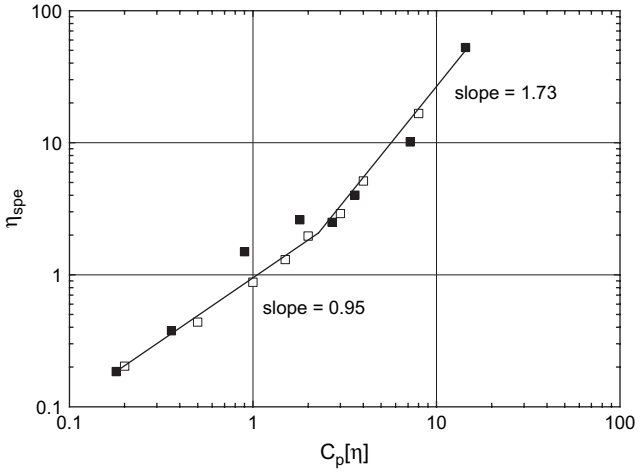

Fig. 5. Evolution of the specific viscosity η_{spe} as a function of $C_p[\eta]$ for solutions of copolymers at 20 °C: (□) PAM-*g*-PNIPA(13); (■) PAM-*g*-PNIPA(46).

(2) Below C^*, the specific viscosity increases almost linearly with the concentration ($\eta_{spe} \sim C^{0.95}$) and above C^* the viscosity starts to increase exponentially. From Fig. 5 we get $\eta_{spe} \sim C^{1.73}$ which is in good agreement with the theoretical exponents 2 and 5/4 predicted for linear polymer chains in θ and good solvents, respectively [23]. As commented by Dobryrin et al. [24], the entangled semi-dilute regime is expected to start at a concentration C_e corresponding to $5 < C_e/C^* < 10$; or at a concentration where the viscosity $\eta_e \cong 50\eta_S$ (above $C_p[\eta] = 10$).

From this study, it appears that the introduction of a few number of long polymer grafts along a polyacrylamide backbone does not modify unduly the rheological behaviour of the parent polymers at low temperature.

3.2.2. PAMH series

Unlike non-ionic macromolecular coils, polyelectrolyte rods start to overlap at very low concentration and the unentangled semi-dilute regime can cover several decades of

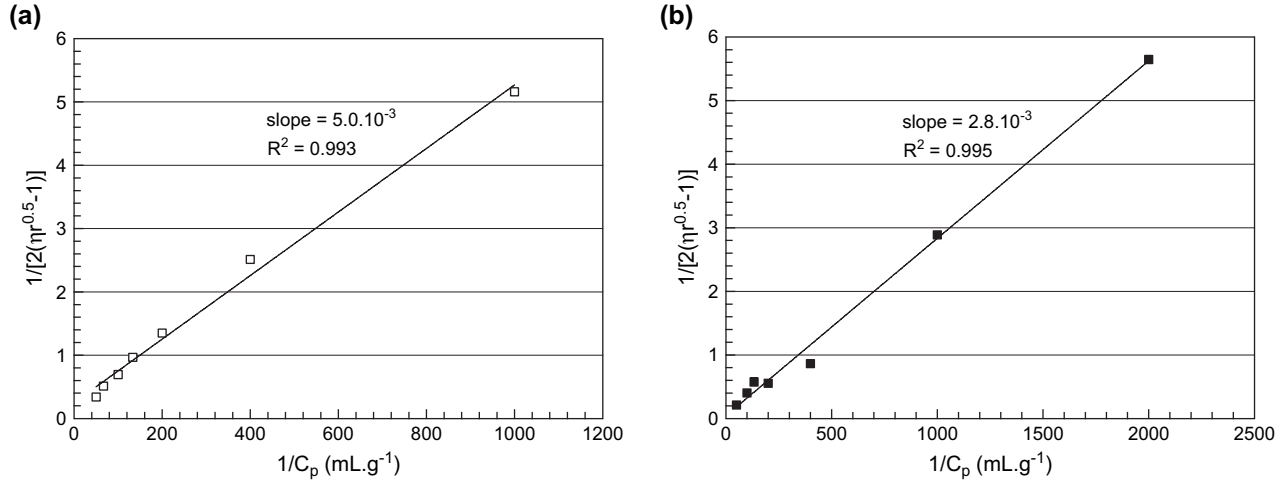

Fig. 4. Fedors plot for copolymer solutions ($T = 20$ °C): (a) PAM-*g*-PNIPA(13) and (b) PAM-*g*-PNIPA(46).

concentration. Here the dilute regime and the overlap concentration are out of scope and we will focus on the entanglement concentration C_e. According to the theoretical work of Dobryrin et al. [24], it is shown that the viscosity of polyelectrolyte solutions, without added salt, follows a unique scaling relation in dilute and unentangled semi-dilute regimes ($\eta_r \sim C_p^{1/2}$) while the concentration dependence increases above C_e, giving rise to $\eta_r \sim C_p^{3/2}$ in the entangled semi-dilute regime.

As shown in Fig. 6, the rheological behaviour of 1-PAMH-*g*-PNIPA(60) in aqueous solution follows the theoretical predictions with scaling exponent of 0.5 and 1.3 in the unentangled and entangled regimes, respectively. We can mention that the lower value obtained in the entangled regime mainly comes from the small number of data in this range.

A common behaviour has been obtained for all the copolymers of this series which have similar weight average molecular weights (see Table 2). This concerns at once the scaling exponents in both the regimes and the entanglement concentrations which are located in the range: $C_e = 10-20\ g\ L^{-1}$. It is also interesting to mention that even in the presence of a high content of neutral material, grafted onto the backbone, the copolymers follow the rules of polyelectrolytes in aqueous solution.

3.3. Thermothickening properties

3.3.1. PAMH-g copolymers

The rheological properties of semi-dilute graft copolymer solutions were investigated as a function of temperature. An example is given in Fig. 7 where the evolution of dynamic moduli (G' and G'') and complex viscosity η^* of an aqueous solution of 1-PAMH-*g*-PNIPA(60) ($C_p = 20\ g\ L^{-1}$) has been followed in the course of heating and cooling. First of all we have to point out that in our experimental conditions ($f = 1$ Hz and heating and cooling rates $= 2\ °C\ min^{-1}$), the properties are perfectly reversible without any noticeable hysteresis as it is shown for the complex viscosity of 1-PAMH-*g*-PNIPA(60). Two temperature domains can be distinguished. At low temperature, i.e. for a temperature lower than the LCST of PNIPA grafts, the side chains are still soluble in water and the viscosity of the copolymer solution is similar to the one expected for the polymer precursor 1-PAMH or for 1-PAMH-*g*-PEO(40) which do not self-associate in these conditions (see Fig. 7).

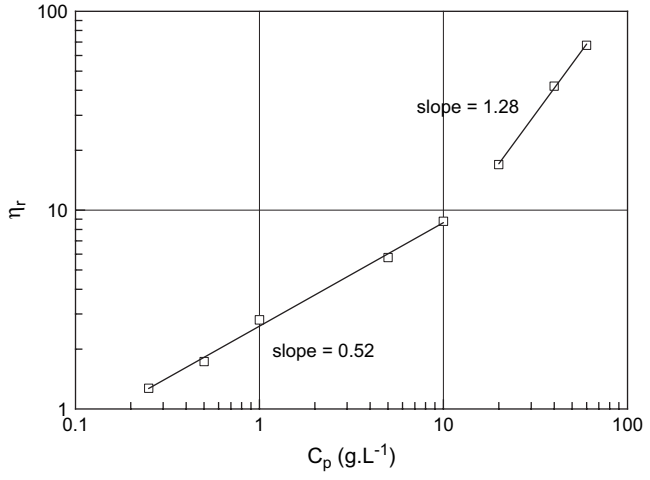

Fig. 6. Relative viscosity η_r as a function of copolymer concentration C_p for solutions of graft copolymer 1-PAMH-*g*-PNIPA(60) at 20 °C.

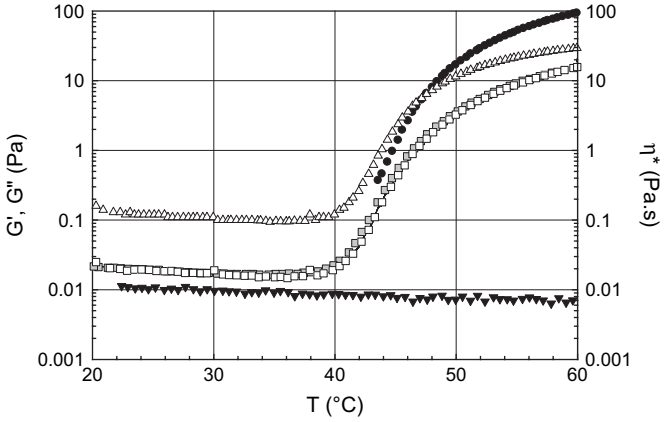

Fig. 7. Temperature dependence of viscoelastic properties ($f = 1$ Hz) for aqueous solutions of graft 1-PAMH ($C_p = 20\ g\ L^{-1}$): 1-PAMH-*g*-PNIPA(60): (●) G'; (△) G'' and η^*((□) heating and (▩) cooling) and 1-PAMH-*g*-PEO(40): (▼) η^*.

The viscosity decreases smoothly between 20 and 38 °C, following an Arrhenius behaviour. At low temperature for 1-PAMH-*g*-PNIPA(60), and at all temperatures for 1-PAMH-*g*-PEO(40), the copolymer solutions are characterised by a low activation energy ($E_a \sim 18\ kJ\ mol^{-1}$), close to the activation energy of the solvent itself ($E_a^{water} \sim 16\ kJ\ mol^{-1}$) which is the main component at this concentration.

Above 38 °C, the self-assembling of PNIPA grafts in micellar junctions gives rise to a strong upturn of the viscosity with temperature. In our experimental conditions ($f = 1$ Hz), the complex viscosity increases over more than 3 decades between 40 and 60 °C. Similarly, the elastic modulus becomes measurable in the course of heating above 44 °C and rapidly surpasses the storage modulus.

Compared to dynamic measurements performed at low deformation in the linear regime, the association process is strongly modified at large deformations. This is exemplified in Fig. 8 where the temperature dependence of the viscosity has been plotted for various shear rates and angular frequencies. By comparison with the low temperature regime where the viscosity is Newtonian, the rheological behaviour becomes rapidly shear thinning above the association temperature. For intermediate temperatures (between 45 and 55 °C), we can notice a deviation from Cox–Merz rule as the complex viscosity becomes lower than the steady-shear viscosity, for experiments performed in similar conditions ($\omega = 1-10\ rad\ s^{-1}$ and $\dot{\gamma}^{-1} = 1-10\ s^{-1}$). Such behaviour has been commonly reported with other associating polymers and more especially with telechelic systems [25,26].

At higher temperature (above 60 °C) the situation is reversed as the steady-shear viscosity decreases with increasing

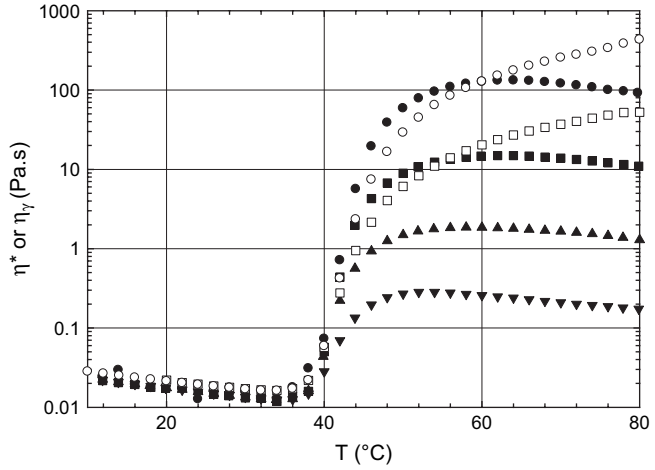

Fig. 8. Influence of shear rate or angular frequency on the thermothickening behaviour of 1-PAMH-*g*-PNIPA(60) solution ($C_p = 25$ g L^{-1}): (●) $\dot{\gamma}^{-1}$ = 1 s^{-1}, (■) 10 s^{-1}, (▲) 100 s^{-1}, (▼) 1000 s^{-1}; (○) $\omega = 1$ rad s^{-1}, (□) 10 rad s^{-1}.

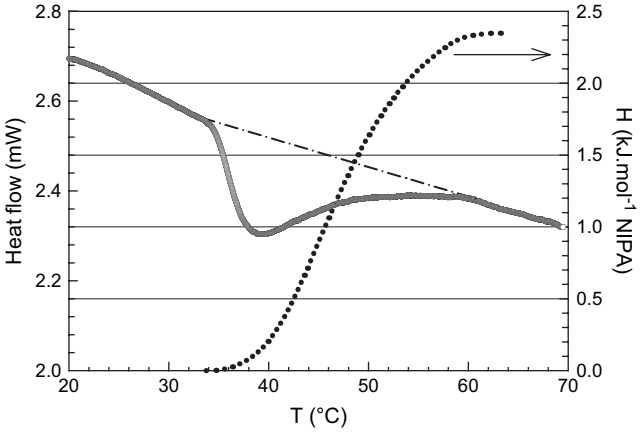

Fig. 9. Heat flow and corresponding enthalpic integral curve *H* (dotted line) as a function of temperature for a solution of 1-PAMH-*g*-PNIPA(60) at $C_p = 20$ g L^{-1}.

temperature while the complex viscosity increases. In these conditions, there is a strong competition between the formation of PNIPA aggregates, driven by the LCST phase separation process, and the disruption of these latter under deformation. For dynamic measurements performed in the linear regime, the strength of the associations and consequently the lifetime of the stickers in the microdomains continuously increase upon heating and likewise with the complex viscosity (see Figs. 7 and 8). For shear experiments, the chains which form bridges between the PNIPA domains are submitted to large extension which tends to pull the stickers outside the aggregates. Consequently the mechanical stress induced by shearing superposes the thermodynamic behaviour of the association process and the net result strongly depends on their relative strength. When the characteristic time of the shear experiment is rather long (low shear rates), in comparison with the lifetime of the stickers, the dynamic behaviour is controlled by the association mechanism: thermodynamic control. In other words the PNIPA grafts self-associate and dissociate sufficiently rapidly to avoid any large stress induced by shear forces. Conversely, at high shear rates, or when the lifetime of the stickers is long compared to the characteristic time of the experiment, the stickers are pulled out from the aggregate by the bridging chains when the latter are fully stretched. In that case the dynamics of the physical network is under mechanical control. This is clearly evidenced at high temperature in Fig. 8, typically above 50–60 °C, where the shear viscosity reaches a maximum and then decreases with the temperature with the same activation energy as the one calculated at low temperature, i.e. before self-assembling. In this high temperature domain, the solution exhibits a shear thinning behaviour with $\eta \sim \dot{\gamma}^{-1}$.

The phase separation of PNIPA from aqueous solutions is an endothermic process [27] which can be evidenced by DSC as shown in Fig. 9. For the solution of 1-PAMH-*g*-PNIPA(60) at $C_p = 20$ g L^{-1}, the very beginning of the transition starts at around 36 °C. The small difference observed between rheology (Fig. 7) and DSC comes from the fact that a few connections between polymer chains are needed to provide a macroscopic answer. Around 60 °C, the phase transition is over and the solution behaves as an associating network. From this experiment the transition enthalpy per NIPA repeat unit of the whole transition process can be determined: $H_t = 2.35$ kJ mol^{-1}. This value of the heat exchange is weaker than the enthalpy determined with similar solution of PNIPA precursor ($H_t = 4.60$ kJ mol^{-1} of NIPA units) and this difference mainly originates from the strong repulsions between polyelectrolyte chains. In that case, we can roughly estimate that about half of PNIPA grafts take part in the dehydration process.

The ^{1}H NMR spectra of 1-PAMH-*g*-PNIPA(60) in D_2O ($C_p = 20$ g L^{-1}) at $T = 20$ and 50 °C are given in Fig. 10.

The peaks located at 3.9 (peak "e") and 1.0 ppm (peak "f") (Fig. 10) correspond to the protons of the isopropyl group of PNIPA grafts: −CH− and $-CH_3$, respectively. With increasing temperature, these peaks broaden and move towards highest chemical shifts. At the same time, the areas of the peaks specific to NIPA progressively decrease above the

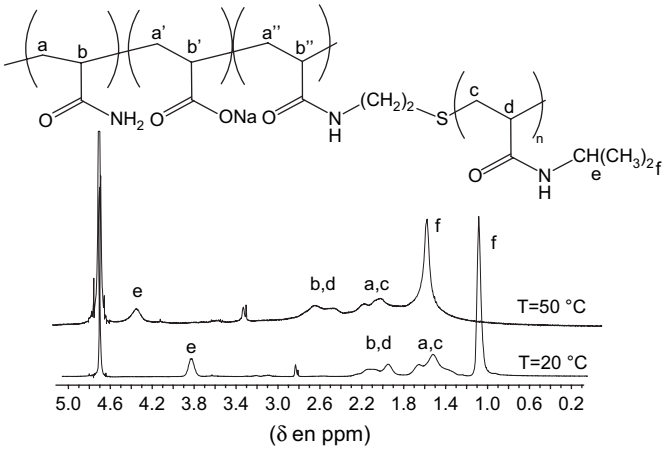

Fig. 10. ^{1}H NMR spectra of a solution of graft copolymer PAMH-*g*-PNIPA at $C_p = 20$ g L^{-1} in D_2O at $T = 20$ and 50 °C.

association temperature. First, we can note that the ratio between the areas corresponding to $-CH_3$ (peak "f") and $-CH-$ (peak "e") is equal to 6 at both temperatures, as expected from the chemical formula. Otherwise, we can calculate that the area of the peak "e", normalized with respect to the signal of the solvent, is 2 times lower at 50 °C compared to its value at 20 °C. Moreover, the ratio between the half-height width of the peak "e" and that of the solvent peak is constant whatever the temperature. This means that the signal from the aggregated NIPA units with low mobility (thus which would give a larger signal) is not detected in our conditions and that consequently the area of the remaining peak corresponds to the protons "e" that keep enough mobility (on the ^1H NMR time scale).

As previously mentioned from DSC experiments, NMR confirms that in the route of the dehydration process, part of PNIPA chains self-associates and looses their mobility forming micellar aggregates to minimize their contact with water. This result is in very good agreement with the previous work of Durand et al. [9] on thermoassociating properties of PAA-*g*-PNIPA derivatives and also with small angle neutron scattering experiments which have been performed with solutions of 1-PAMH-*g*-PNIPA(60). An example is given in Fig. 11 at a copolymer concentration $C_p = 80\ g\ L^{-1}$.

Qualitatively, such scattering curve points out the formation of an organized structure at high temperature with a correlation peak centred at q_{max} which is inversely proportional to the average distance between PNIPA domains ($d \sim q_{max}^{-1}$). Quantitatively, the scattering patterns obtained with 1-PAMH-*g*-PNIPA(60) solutions have been analysed in detail [28] using a micellar model which considers PNIPA side chains aggregating into spherical micellar cores surrounded and interconnected by PAMH backbones. The details of this model, which assumes that the microdomains interact between them with a hard sphere potential, are given in Refs. [29,30].

The quantitative adjustment of the scattering data (see Fig. 11) allows to extrapolate structural informations like the fraction of PNIPA which participates in the formation of micelles ($f = 0.55$), the size of the PNIPA cores ($R_0 = 75$ Å) or the average aggregation number ($N_{ag} = 135$). Assuming a weak concentration dependence of these structural parameters [28], we can notice that there is a good agreement between the different techniques (DSC, NMR and SANS) concerning the fraction of PNIPA embedded inside the aggregates (around 50%).

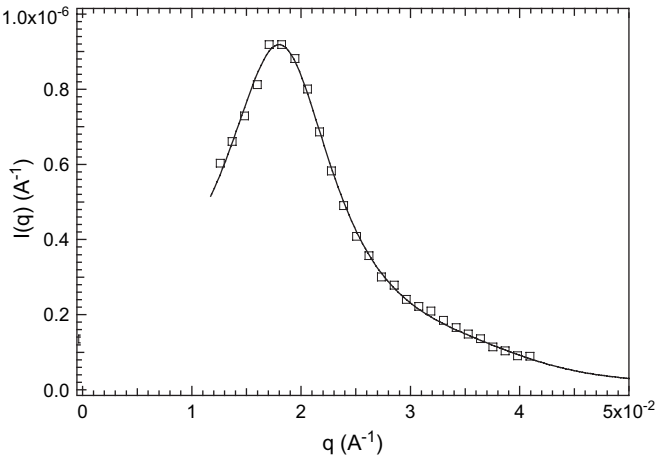

Fig. 11. Scattering profile of 1-PAMH-*g*-PNIPA(60) in D_2O at $C_p = 80\ g\ L^{-1}$ and $T = 60$ °C. Experimental data (symbols) and model fitting (line).

The associating behaviour described with the solutions of 1-PAMH-*g*-PNIPA(60) is very general and representative of PNIPA graft copolymers. For instance we have plotted in Fig. 12 the thermoresponsive signature of copolymers issued from 2-PAMH.

By comparison with the previous discussion, this picture illustrates the influence of copolymer concentration on the responsive behaviour with a weakening of the properties and a shift of the association temperature with decreasing concentration. The main reasons are:

(1) an increase of the electrostatic repulsions taking place between the polymer backbones (decrease of the self-screening),
(2) a decrease of the balance between inter- and intramolecular associations.

As a matter of fact, the network properties strongly depend on the relative proportion between bridges, loops and dangling chains and a critical polymer concentration is needed to reach the percolation threshold. Using the criteria of the percolation theory, this concentration was estimated around $C_{gel} = 3\ g\ L^{-1}$ for solutions of 1-PAMH-*g*-PNIPA(60) [28] and must be a little bit lower for 2-PAMH-*g*-PNIPA(50) (see Fig. 12).

3.3.2. PAM-g-PNIPA copolymers

The rheological behaviour of graft PAMs prepared by copolymerisation is given in Fig. 13.

The comparison between the two non-ionic polymers first illustrates the influence of the grafting ratio on the thermothickening behaviour which becomes sharper with increasing

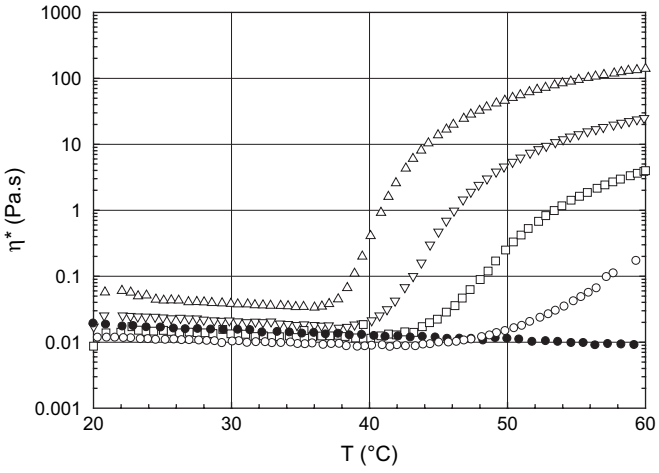

Fig. 12. Temperature dependence of complex viscosity ($f = 1$ Hz) of aqueous solutions of graft 2-PAMH: (a) 2-PAMH-*g*-PNIPA(50): (○) $C_p = 3\ g\ L^{-1}$; (□) $6\ g\ L^{-1}$; (▽) $12\ g\ L^{-1}$; (△) $C_p = 24\ g\ L^{-1}$; (b) 2-PAMH-*g*-PDMA(70): (●) $C_p = 10\ g\ L^{-1}$.

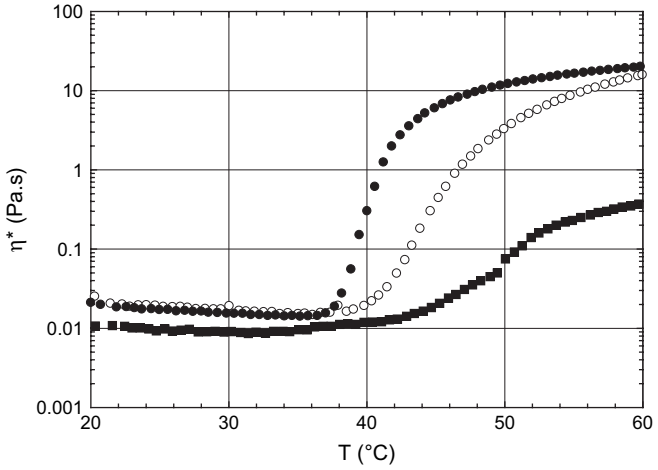

Fig. 13. Complex viscosity η^* as a function of temperature for PNIPA graft copolymers solution at $C_p = 20\ g\ L^{-1}$: (■) PAM-*g*-PNIPA(13); (●) PAM-*g*-PNIPA(46); (○) 1-PAMH-*g*-PNIPA(60).

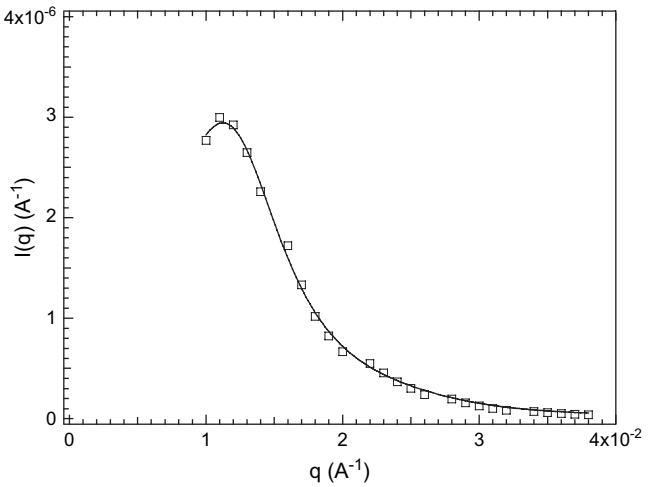

Fig. 14. Scattering profile of PAM-*g*-PNIPA(46) in D_2O at $C_p = 80\ g\ L^{-1}$ and $T = 60\ °C$. Experimental data (symbols) and model fitting (line).

PNIPA content. While the viscosity of PAM-*g*-PNIPA(46) starts to increase gradually above 36–37 °C, the thermothickening signature of PAM-*g*-PNIPA(13) evidences the strong heterogeneity of the sample. As a matter of fact, the viscosity increases with temperature following various steps, at least two, with a first one at low temperature ($T \cong 33\ °C$) and a second one a little bit above 40 °C. Taking into account the characteristics of the copolymerisation discussed previously, the low temperature process can be correlated to copolymer chains containing a high fraction of PNIPA grafts which were prepared during the last stage of the copolymerisation. Once again there is a clear correlation between structure and properties of the copolymers and we can assume that PAM-*g*-PNIPA(46) is much more homogeneous even if the composition drift of the chains has to be taken into account in the association phenomenon.

In Fig. 13, the viscosity of 1-PAMH-*g*-PNIPA(60) has also been plotted for comparison with PAM-*g*-PNIPA(46). Interestingly, the two copolymers exhibit exactly the same viscosity and temperature dependence in the low temperature range despite the important differences in chemical nature and molecular weight. Nevertheless, it appears that the non-ionic sample starts to self-assemble at a lower temperature, despite a smaller PNIPA content, and gives rise to a sharper thickening effect (higher slope $\Delta\eta/\Delta T$) at around 40 °C.

This macroscopic behaviour can be correlated to the absence of electrostatic repulsions between PAM backbones which favours the self-assembly of PNIPA grafts into hydrophobic domains. Similar results were also obtained by DSC performed with a PAM-*g*-PNIPA(46) solution at $C_p = 20\ g\ L^{-1}$. In that case the phase transition begins at 34 °C and the transition enthalpy per NIPA unit reaches $3.63\ kJ\ mol^{-1}$. By comparison with the enthalpy of free PNIPA, this would correspond to a dehydration of 80% of PNIPA grafts in the case of the non-ionic polymer, instead of 50% for the polyelectrolyte sample. Finally, some complementary studies have been performed by SANS in order to investigate the local structure of PAM-*g*-PNIPA(46) in aqueous solution (Fig. 14).

Compared to with the SANS profile of 1-PAMH-*g*-PNIPA(60) given in Fig. 11, PAM-*g*-PNIPA(46) performed at the same concentration, shows a higher intensity for the scattering peak and a shift of its position towards lower q values. The qualitative conclusion is that the non-ionic PAM-*g*-PNIPA(46) forms larger aggregates at high temperature in aqueous solution. By applying the core–shell model previously described, the fit of the experimental data gives $f = 0.69$, for the fraction of PNIPA embedded into the micelles, $R_0 = 120$ Å for the size of PNIPA aggregates and $N_{ag} = 523$.

On the basis of these parameters, we can conclude that for comparable amount of responsive grafts, the polyelectrolyte backbones introduce electrostatic repulsions which are opposed to the association mechanism driven by PNIPA grafts. This repulsive component, which also makes the system more stable (smaller aggregates), is responsible for the broadening of the thermothickening effect observed at moderate concentration.

3.3.3. Salt and pH effect on thermoassociating properties

Depending on their use, the rheological properties of associating polymers have to be considered in a more real environment taking into account the pH and the presence of added salts. This is shown in Fig. 15 where the thermothickening properties of graft copolymers are compared in water and in moderate concentration of sodium chloride ($0.1\ mol\ L^{-1}$).

From a general point of view, addition of inorganic salts is known to generally decrease the solubility of LCST polymers in aqueous media as they behave as competitors towards water molecules. Each salt produces different effects, depending on the nature of anions and cations, and the magnitude of the salting-out effect is generally scaled according to the Hoffmeister series with reference to the effect of salt on the solubility of proteins in water. In the present case we use sodium chloride which is known to decrease moderately the solubility of LCST polymers. This can be directly observed in Fig. 15 where the addition of NaCl decreases the association process of about

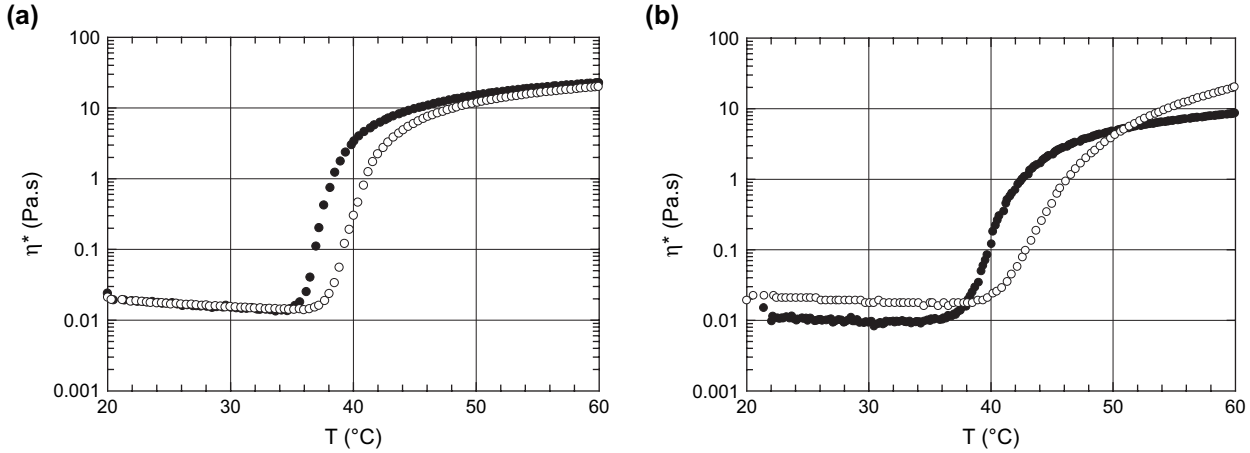

Fig. 15. Influence of added salt on the temperature dependence of complex viscosity for (a) PAM-*g*-PNIPA(46) at $C_p = 20\ g\,L^{-1}$: (○) H_2O; (●) [NaCl] = 0.1 mol L^{-1} and (b) 1-PAMH-*g*-PNIPA(60) at $C_p = 20\ g\,L^{-1}$: (○) H_2O; (●) [NaCl] = 0.1 mol L^{-1}.

$\Delta T = 4-5$ °C for the two copolymers. For PAM-*g*-PNIPA(46), this is the only effect as the solubility and the conformation of the PAM backbone are not modified in these conditions. In other words, the two curves obtained with and without salt can be superposed using a simple shift along the temperature axis.

The situation is different for 1-PAMH-*g*-PNIPA(60) which is polyelectrolyte and consequently very sensitive to ionic strength. In the presence of added salt, we observe:

(1) a shift of the thermothickening at lower temperature. This is mainly the influence of salt on the thermodynamic properties of PNIPA grafts;
(2) a decrease of the viscosity at low temperature. This comes from the conformational ''collapse'' of the polyelectrolyte backbone due to the screening effect of salt;
(3) an increase of the thermothickening behaviour ($\Delta\eta/\Delta T$). Again, this is attributed to the screening of the electrostatic repulsions taking place between the PAMH backbones;
(4) a decrease of the viscosity at high temperature. This observation can be correlated to the collapse of the polyelectrolyte chain (increase of the ratio between loops and bridges) and certainly to an increase of the size of PNIPA aggregates (decrease of the total number of physical crosslinks).

By comparison, the effect of pH reported in Figs. 16 and 17 is much more pronounced between graft PAM and PAMH copolymers.

In these conditions (pH = 2–7), the ionic strength is low and does not influence the thermodynamic behaviour of PNIPA grafts. As PAM is non-ionic, its conformation remains unchanged in this range of pH and likewise with the thermothickening properties of PAM-*g*-PNIPA(13).

Conversely, the temperature dependence of the 1-PAMH-*g*-PNIPA(60) solution is dramatically modified between pH = 6 and 2 (see Fig. 17).

This can be understood taking into account the weak polyelectrolyte character of the copolymer. At low temperature

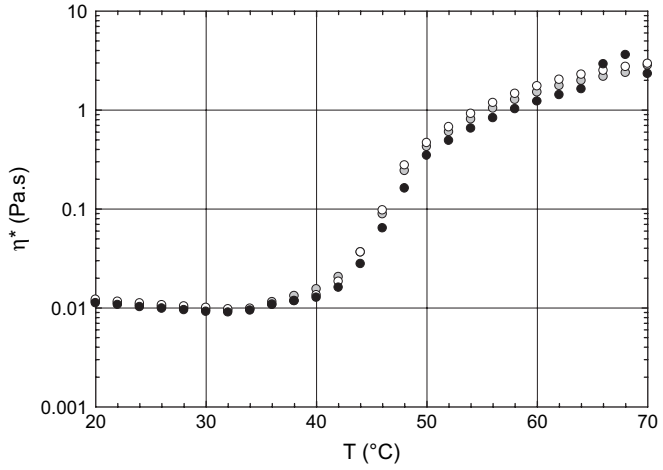

Fig. 16. Influence of pH on the temperature dependence of complex viscosity for PAM-*g*-PNIPA(13) at $C_p = 25\ g\,L^{-1}$: (○) pH = 7; (●) pH = 3.5; (●) pH = 2.

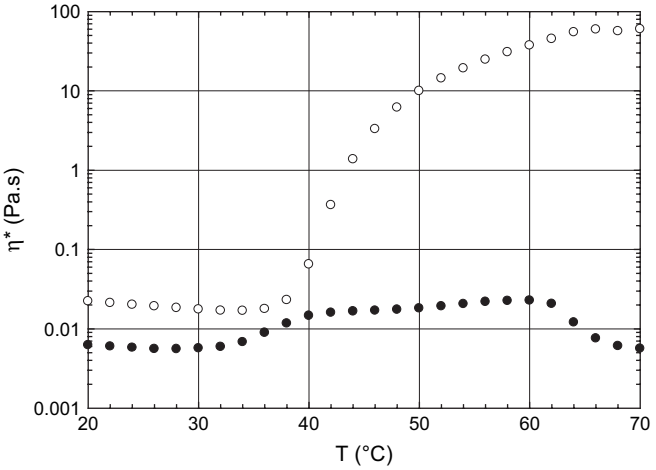

Fig. 17. Influence of pH on the temperature dependence of complex viscosity for: 1-PAMH-*g*-PNIPA(60) at $C_p = 25\ g\,L^{-1}$: (○) pH = 6; (●) pH = 2.

and low pH, the PAMH backbone is not charged and its conformation is much less extended compared to pH = 6. The viscosity of the copolymer solution is divided by 4, between pH = 6 and 2, and this can be correlated to the collapse (deswelling) of the chain. By increasing the temperature, the solution at pH = 2 starts to self-associate earlier but the increase of viscosity remains very small in these conditions and eventually gives rise to a phase separation at higher temperature.

The main difference between PAM and PAMH at pH = 2 is that this latter is able to develop specific interactions (hydrogen bonds) between carboxylic groups and acrylamide and/or NIPA units [31]. The PAMH copolymers exhibit consequently a lower solubility in aqueous media at low pH and become insoluble at high temperature when the attractive interactions overcome the excluded volume interactions. A phase separation was also described by Durand and Hourdet [8] in the case of poly(acrylic acid)-*g*-PNIPA solutions at low pH but in that case it was clearly a complex coacervation driven by hydrogen bonding between the polyacrylic acid backbone and the PNIPA grafts.

4. Conclusion

The purpose of this work was to prepare a series of graft copolymers based on polyacrylamide using two different routes – grafting onto and grafting through – and to compare the thermoassociating properties of PNIPA derivatives in aqueous media. We have shown that the ''grafting onto'' method was clearly the best way to control the primary structure of the copolymers and more particularly the size and the molecular weight distribution of the backbone as well as the distribution of grafts along the main chain. Nevertheless, the grafting of α-amino-terminated grafts requires acrylic acid units in the backbone and these ionic groups, even at low content, introduce electrostatic repulsions and some environmental sensitivity which can affect the self-assembling properties.

Conversely the ''grafting through'' method allows to obtain non-ionic copolymers but their primary structure is far to be controlled. The main problem comes from the important difference of reactivity between acrylamide and macromonomers which gives rise to a large drift of composition during the reaction. Some improvement could be made by stopping the reaction at lower conversion or more reasonably by feeding continuously with acrylamide in order to keep the monomer ratio constant during the copolymerisation.

At room temperature and neutral pH, the copolymers mainly behave in aqueous solution as their linear precursors. Even with a high proportion of neutral side chains (40–70 wt.%) the graft PAMHs follow the scaling relations predicted for polyelectrolytes and the electrostatic repulsions are also clearly evidenced upon heating above the phase transition of PNIPA grafts. As a matter of fact, the thermothickening mechanism is controlled by the competition between PAMH/PAMH repulsions and PNIPA/PNIPA attractions. This balance can be modified by screening the electrostatic interactions: increasing the copolymer concentration, adding salt or decreasing the degree of ionisation (lowering the pH). Nevertheless we have shown that if PNIPA graft polyelectrolytes exhibit very good thermothickening properties and stability in water, they progressively behave as non-ionic copolymers in the presence of salt and become unstable at low pH (phase separation). By comparison, the non-ionic PAM copolymers also exhibit good thermothickening properties in aqueous solution but with a lower sensitivity and a higher stability towards environmental conditions. So despite the weak control of the primary structure, we can conclude that ''grafting through'' is an interesting alternative to prepare self-assembling graft copolymers with targeted chemistry.

By using PNIPA, PDMA or PEO grafts, our initial purpose was to modulate the strength of associations between grafted copolymers and silica nanoparticles in aqueous media. The results of this study on hybrid hydrogels will be presented in a forthcoming article.

Acknowledgements

The authors want to thank Sarah Marais for her help in copolymer synthesis, Dr. Guylaine Ducouret (PPMD, ESPCI, Paris) for her experienced advices on performing rheological measurements on associating polymers and Dr. Annie Brûlet (LLB, CEA, Saclay) for her helpful guidance in neutron scattering experiments.

References

[1] Responsive gels: volume transitions I and II. Adv Polym Sci 1993:109–10.
[2] Bromberg L. Macromolecules 1998;31:6148.
[3] Durand A, Hervé M, Hourdet D. In: Mc Cormick CL, editor. ACS symposium series, vol. 780; 2000. p. 181.
[4] Hourdet D, L'Alloret F, Audebert R. Polymer 1997;38:2535.
[5] Hourdet D, L'Alloret F, Durand A, Lafuma F, Audebert R, Cotton J-P. Macromolecules 1998;31:5323.
[6] Haraguchi K, Takeshita T. Macromolecules 2002;35:10162.
[7] Feil H, Bae Han Y, Feijen J, Kim SW. Macromolecules 1993;26:2496.
[8] Durand A, Hourdet D. Macromol Chem Phys 2000;201:858.
[9] Durand A, Hourdet D, Lafuma F. J Phys Chem B 2000;104:9371.
[10] Portehault D, Petit L, Pantoustier N, Ducouret G, Lafuma F, Hourdet D. Colloids Surf A 2006;278:26.
[11] Sudor J, Barbier V, Thirot S, Godfrin D, Hourdet D, Millequant M, et al. Electrophoresis 2001;22:720.
[12] Durand A, Hourdet D. Polymer 1999;40:4941.
[13] Bokias G, Durand A, Hourdet D. Macromol Chem Phys 1998;199:1387.
[14] Shibanuma T, Aoki T, Sanui K, Ogata N, Kikuchi A, Sakurai Y, et al. Macromolecules 2000;33:444.
[15] Jewrajka SK, Mandal BM. Macromolecules 2003;36:311.
[16] Jewrajka SK, Mandal BM. J Polym Sci Part A Polym Chem 2004;42:2483.
[17] Thomas DB, Sumerlin BS, Lowe AB, McCormick CL. Macromolecules 2003;36:1436.
[18] Lloyd DR, Burns CM. J Polym Sci Polym Chem Ed 1979;17:3459.
[19] Halverson F, Lancaster JE, O'Connor MN. Macromolecules 1985;18:1139.
[20] Magny B, Lafuma F, Iliopoulos I. Polymer 1992;33:3151.
[21] Fedors RF. Polymer 1979;20:225.
[22] Grigorescu G, Kulicke W-M. Adv Polym Sci 2000;152:1.

[23] Colby RH, Rubinstein M. Macromolecules 1990;23:2753.
[24] Dobryrin AV, Colby RH, Rubinstein M. Macromolecules 1995;28: 1859.
[25] Annable T, Buscall R, Ettelaie R, Whittlestone D. J Rheol 1993;37(4): 695.
[26] Tripathi A, Tam KC, McKinley GH. Macromolecules 2006;39:1981.
[27] Schild HG, Tyrell DA. J Phys Chem 1990;94:4352.
[28] Petit L, Bouteiller L, Brûlet A, Lafuma F, Hourdet D. Langmuir 2007;23: 147.
[29] Barbier V, Hervé M, Sudor J, Brûlet A, Hourdet D, Viovy J-L. Macromolecules 2004;37:5682.
[30] Hourdet D, Gadgil J, Podhajecka K, Badiger MV, Brûlet A, Wadgaonkar PP. Macromolecules 2005;38:8512.
[31] Bokias G, Staikos G, Iliopoulos I. Polymer 2000;41:7399.